JOC The Journal of Organic Chemistry

ARTICLE

pubs.acs.org/joc

Synthesis and Optical Properties of Acidochromic Amine-Substituted Benzo[*a*]phenazines

Prachi Singh, Abhishek Baheti, and K. R. Justin Thomas*

Organic Materials Lab, Department of Chemistry, Indian Institute of Technology Roorkee, Roorkee-247 667, India

Supporting Information

ABSTRACT:

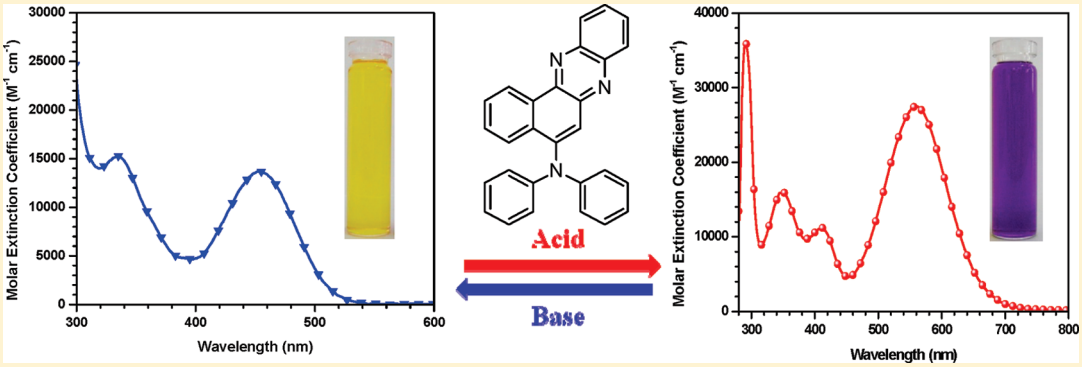

A new series of alkylamine- or arylamine-substituted benzo[*a*]phenazines have been synthesized from 1,2-naphthoquinones by employing simple sequential Michael-type addition with a variety of primary and secondary amines and the condensation reaction of the resulting amine-substituted 1,2-naphthoquinones with *o*-phenylenediamine. They exhibited absorption peaks originating from the charge transfer transition between the amine and pyrazine segments and benzo[*a*]phenazine localized $\pi-\pi^*$ transitions. Although the absorption spectra of the dyes were not significantly influenced by the nature of the solvents, addition of TFA led to a prominent red-shift in the absorption spectra owing to the protonation at the quinoxaline segment which enhanced the electron-accepting ability. The qualitative trends observed in the optical properties and acidochromism were supported by density functional theoretical computations. The dyes displayed positive solvatochromism in the emission spectra suggestive of a more polar excited state. The dyes were also characterized by a quasi-reversible reduction couple originating from the pyrazine segment which underwent shifts corresponding to electron-donating strength of the amine segment.

INTRODUCTION

Organic materials featuring donor-π-bridge-acceptor architecture have continued to attract wide attention owing to their potential applications as red emitting charge transporters in organic light-emitting devices (OLED),[1] as semiconductors in thin film transistors (TFT),[2] and as sensitizers in excitonic solar cells (DSSC).[3] These dipolar compounds are also attractive due to their application in the sensor industry.[4] In a suitably designed donor−acceptor compound, modulation of the donor or acceptor property by the interaction of analyte leads to the signal amplification. These dipolar compounds are typically constructed using an aromatic π-linker which facilitates the interaction between the donor and acceptor moieties.[5] Frequently, triarylamines[6] or heterocyclic bases such as carbazole,[7] phenothiazine,[8] etc. were used as donor fragments, while depending on the targeted applications electron-accepting moieties such as dicyanovinyl,[9] cyanoacrylic acid,[10] oxadiazole,[11] benzothiadiazole,[12] pyrazine/quinoxaline,[13−15] and their aromatic fused analogs served as an acceptor group. Particularly, the triarylamine and oxadiazoles, quinoxalines or dicyanovinyl conjugates have been demonstrated to function as dual transport materials with promising emission characteristics.[9,11,13] Pyrazines or quinoxalines are electron-accepting moieties and have been exploited for the construction of electron-transporting materials suitable for OLED fabrication.[13−15] In addition, integration of electron-donating arylamines/groups with the pyrazine or quinoxaline structure has been demonstrated to produce useful dipolar materials with balanced dual charge transport characteristics.[16] However, the triarylamine donor and cyanoacrylic acid acceptor based organic dyes have been widely applied as sensitizers in dye-sensitized solar cells with exceptional light harvesting peroperties.[10]

The functional properties of the donor−acceptor compounds are highly dependent on the nature of the aromatic conjugation that unites the donor and acceptor fragments. It has been observed that the oligothiophene segments function as effective molecular wire for electronic mediation when compared to the corresponding oligophenylene units owing to the associated reduced aromaticity, electron richness, and

Received: April 27, 2011
Published: June 06, 2011

Chart 1. Structures of the Amine-Substituted Benzo[*a*]phenazines

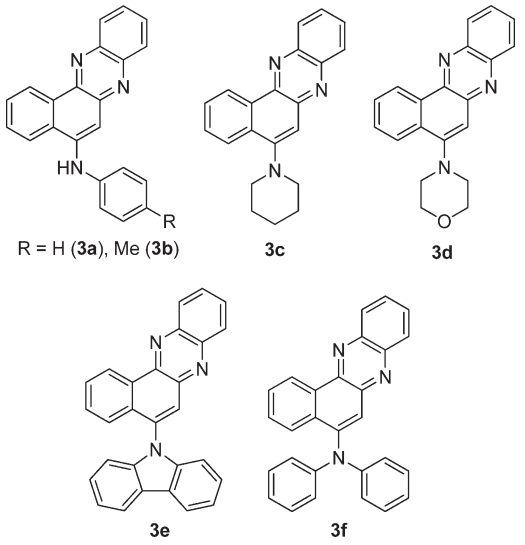

planarity.[17] Also, the replacement of the biphenyl moiety with a fluorene unit has also been found to exert beneficial role on the desired electro-optical properties. Besides this, the strategy of forming a rigid polyaromatic planar heterocyclic nucleus by the fusion of donor and acceptor units together has also received immense attention in recent years due to their special electro-optical properties originating from the low band gap of such architectures.[18] The fused heterocyclic structures inherit rigidity and favorable highest occupied and lowest unoccupied molecular orbitals. These characteristics are beneficial for the red-shifted emission and balanced dual charge transport properties.

Polyaromatic fused heterocycles such as fluorenoquinoxaline,[19] pyrenoquinoxaline,[19] acenaphtho[1,2-*b*]quinoxaline,[20] [1,2,5]thiadiazolo[3,4-*g*]quinoxaline,[21] thieno[3,4-*b*]pyrazine,[22] pyrroloquinoxaline,[23] and indoloquinoxaline[24] based functional materials have been developed and shown to possess interesting electro-optical properties. However, to the best of our knowledge, the benzo[*a*]phenazine derivatives containing amino functionality have not been studied in detail despite their biological applications.[25] Pyrazine/quinoxaline and amine conjugates with extended π-linkers have been reported in the literature.[16] The donor−acceptor interaction in such molecules is mainly dependent on the nature of the conjugating unit. On the contrary, direct attachment of the amine functionality on the aromatic nucleus fused with the pyrazine/quinoxaline segment is believed to play concerted role on the electro-optical properties owing to the strong donor−acceptor interaction facilitated by the precise placement of the constituent units in a planar arrangement. In this work, we report the synthesis and optical properties of a series of amine substituted benzo[*a*]phenazine derivatives (Chart 1). Since the amine substituted benzo[*a*]phenazines are donor−acceptor compounds, depending on the nature of the amine the charge transfer transition might be modulated. In order to study the impact of the nature of the amine on the optical properties, we have investigated the derivatives derived from both the primary and secondary amines. Similarly, the alkyl and aryl amines were used to elucidate the changes in the optical properties arising due to the variation in the donor strength and π-conjugation. Additionally, specific interaction of the amine or

Scheme 1. General Synthetic Scheme Employed for the Preparation of the Dyes 3a−f

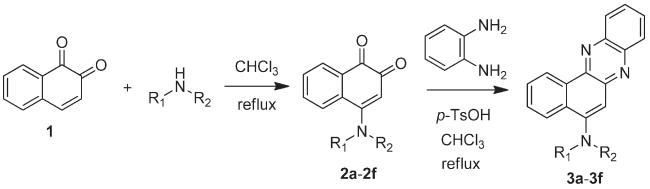

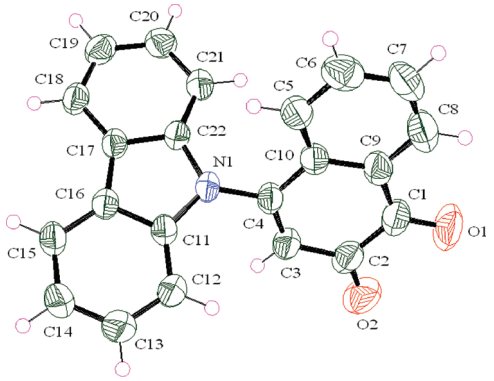

Figure 1. ORTEP plot (50% thermal ellipsoids) of the compound **2e**.

pyrazine unit with metals may be exploited for sensor-type applications. In order to explore this feasibility, we have also investigated the sensitivity of these molecules toward acids which could be considered as model studies. Chromophores changing color on interaction with acids, termed as acidochromism, have been studied in detail in recent years owing to its importance in the sensor industry.[26]

RESULTS AND DISCUSSION

Synthesis and Characterization. The syntheses of the dyes were accomplished by a two-step process as outlined in Scheme 1. In the first step, 1,2-naphthoquinone was treated with the corresponding primary or secondary amine in chloroform to yield the 4-substituted 1,2-naphthoquinone derivatives (**2a**−**f**). The reaction itself proceeded at room temperature; however, gentle heating at 60 °C significantly reduced the reaction time. Both aryl- and alkylamines were found to react in a facile manner with 1,2-naphthoquinone. Reactions of primary amines with 1,2-naphthoquinone have been reported to yield either 4-substituted derivatives or anils.[27] To the best of our knowledge, the reactions of secondary amines with 1,2-naphthoquinone have not been explored. The amine-substituted naphthoquinones were conveniently converted to benzo[*a*]phenazines (**3a**−**f**) by refluxing with *o*-phenylene diamine in chloroform in the presence of a catalytic amount of *p*-toluene sulfonic acid. Attempts to isolate piperidine derived naphthoquinone, **2d** in pure form for analytical measurements were unsuccessful. However, the desired benzo[*a*]phenazine, **3d** was easily obtained in a one-pot reaction from 1,2-naphthoquinone, piperidine and 1,2-diaminobenzene. Later, we confirmed that this one-pot two-step methodology can be employed for all derivatives (**3a**−**f**). The second strategy is very convenient as it excludes the isolation of naphthoquinone intermediates by the tedious column chromatographic separations. The dyes were characterized by ^{1}H and ^{13}C NMR, and high

dx.doi.org/10.1021/jo200857p |*J. Org. Chem.* 2011, 76, 6134–6145

resolution mass spectral methods. The dyes are yellow or brown (**3b**) in the solid state and freely soluble in common organic solvents, such as dichloromethane, $CHCl_3$, THF, toluene, and cyclohexane and insoluble in alcohols.

The single crystal X-ray structure determination of an intermediate (**2e**) was performed (Figure 1) which confirmed the presence of the proposed structure for the naphthoquinone derivatives. The C−N bond distances within the carbazole nucleus and the one connecting carbazole to the naphthoquinone moiety are similar (1.40−1.41 Å) and fall close to the average aromatic C−N bond distance (C−N single bond 1.47 Å; double bond 1.34 Å; aromatic 1.43 Å). This indicates that the lone pair on the carbazole nitrogen is delocalized into the naphthoquinone segment probably due to the electron-accepting tendency of the diketone moiety. The carbazole and the naphthoquinone segments are twisted from one another with an interplanar angle of 60.23 (02)°.

Photophysical Properties. Absorption spectra of the dyes recorded in the toluene solutions are displayed in Figure 2 and the relevant parameters are compiled in Table 1. All of the compounds exhibited a broad and moderately intense absorption band >400 nm attributable to the electronic transition originating from the π-molecular orbitals. The peak position of this band assumes a trend (**3e** < **3c** < **3d** < **3a** < **3b** < **3f**) reflecting the impact of the amine segment on the electronic properties and is not altered by the nature of the solvent used in the measurement. The arylamine derivatives (**3a**, **3b**, and **3f**) showed the red-shifted absorption profiles when compared to the alkylamine derivatives (**3c** and **3d**) and the compound containing carbazole (**3e**). The diphenylamine derivative (**3f**) possesses the longest wavelength absorption while the carbazole derivative (**3e**) shows the shortest wavelength absorption in the series. These observations cannot be explained by assuming charge transfer nature for the transition and the trend is not matching with the donor strength of the amine segments. On the basis of pK_b, the amines are arranged in the decreasing order of donor strength as: piperidine (pK_b = 2.8) > morpholine (pK_b = 5.6) > aniline (pK_b = 9.4) > diphenylamine (pK_b 13.2) > carbazole (pK_b = ~18.9).[28] So the longer wavelength absorption peak in the series must be observed for the piperidine (**3c**) and morpholine (**3d**)

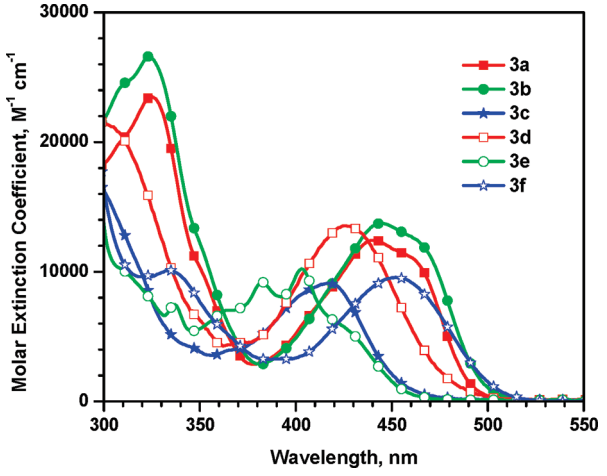

Figure 2. Absorption spectra of the dyes (**3a**−**f**) recorded in toluene.

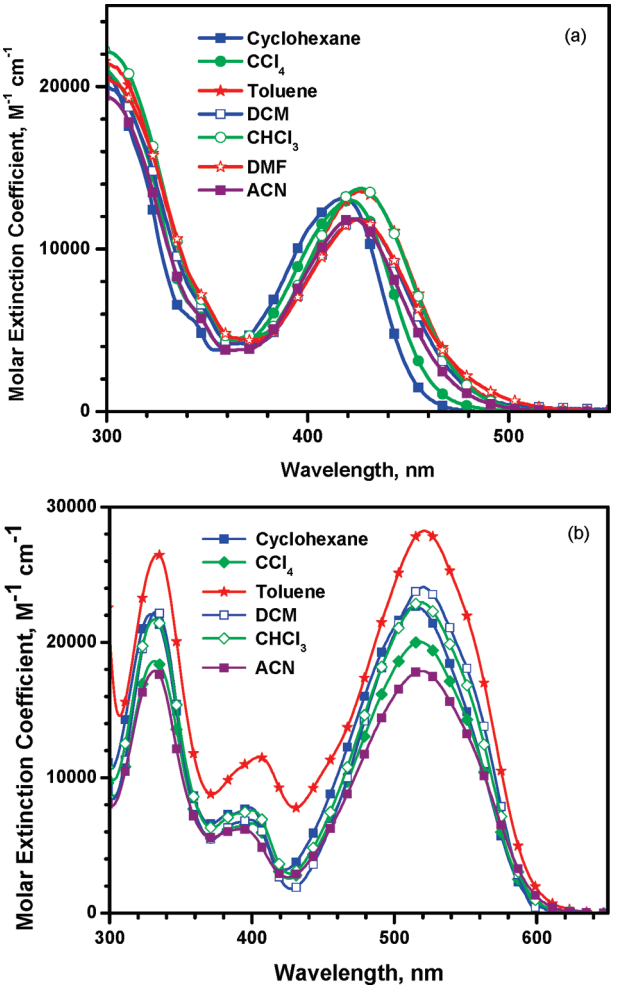

Figure 3. Absorption spectra of **3d** recorded in different solvents (a) before and (b) after the addition of TFA.

Table 1. Optical Data of the Dyes Recorded for Toluene Solutions

dye	λ_{abs}, nm (ε_{max}, 10^3 $M^{-1}cm^{-1}$)			λ_{em}, nm (Φ_F, %)
	TOL	TOL + TFA (10 equiv)	TOL + TFA (1000 equiv)	TOL
3a	441 (12.4), 325 (23.5), 287 (20.9)	520 (18.2), 395 (6.2), 330 (21.1)	522 (15.1), 396 (6.2), 323 (17.2)	504 (18)
3b	445 (14.8), 324 (26.6), 287 (22.9)	525 (18.7), 392 (6.3), 329 (21.9)	522 (16.9), 396 (6.9), 323 (19.3)	515 (16)
3c	419 (9.1), 285 (20.8)	500 (10.5), 404 (5.5), 321 (12.3)	497 (15.9), 413 (7.5)	521 (26)
3d	426 (13.6), 277 (34.42)	515 (23.1), 400 (7.5), 331 (24.6)	521 (21.2), 405 (11.5), 333 (26.5)	533 (25)
3e	403 (10.2), 383 (9.2), 286 (46.7)	596 (11.1), 433 (8.6), 335 (11.9)	449 (17.9)	492 (22)
3f	452 (9.6), 335 (10.1), 286 (38.8)	557 (13.6), 411 (3.2), 349 (8.4)	560 (13.0), 414 (5.4)	543 (27)

dx.doi.org/10.1021/jo200857p |*J. Org. Chem.* 2011, 76, 6134–6145

derivatives. But the red-shifted absorption profiles observed for the arylamine derivatives (**3a**, **3b**, and **3f**) is suggestive of the involvement of conjugative delocalization. Extended conjugation present in the above derivatives may lead to a red-shifted absorption. On the contrary, the blue-shifted profile observed for **3e** may be attributed to the retardation of electronic delocalization caused by the twist between the carbazole and benzo[*a*]phenazine segments (vide supra).[29] In view of these observations, it may be argued that the prominent absorption in the arylamine derived compounds is mainly originating from the $\pi-\pi^*$ transition or having significant contribution from the $\pi-\pi^*$ transition. The carbazole derivative, **3e** displays multiple overlapping peaks characteristic of a vibronic pattern which attests its rigid structure when compared to the other compounds.

Solvatochromism for the donor−acceptor compounds largely originate due to the difference in the dipole moments of the molecule in the ground state and the excited states and its stabilization by solvent molecules involving various specific interactions such as dipole−dipole, hydrogen bonding, and solvation. All of the dyes studied in this work exhibited a slight red-shift for the absorption peak when recorded in polar solvents such as dichloromethane, acetonitrile and dimethylformamide. A representative variation of absorption spectra with polarity of the solvents is illustrated in Figure 3 for the dye **3d**. The effect of the solvent on the absorption peak saturated quickly on increasing the polarity of the solvent and the dyes generally showed closely resembling absorption profiles in the solvents such as chloroform, dichloromethane, acetonitrile, and dimethylformamide. This suggests a less polar ground state which will be less effectively solvated by the polar solvents. More solvation induced stabilization could lead to a blue shift for the absorption profiles in the polar solvents.[30]

The absorption spectra of the dyes bathochromically shifted on addition of trifluoroacetic acid (TFA). Initially, on addition of TFA, the higher wavelength band at <500 nm was gradually replaced by a red-shifted peak at >500 nm. A representative illustration of changes for **3a** in the absorption profile on incremental addition of TFA is shown in Figure 4. The red-shifted absorption peak realized for the dyes in the presence of TFA is attributed to the protonated species. It is possible that the protonation of pyrazine segment occurs in the presence of TFA and generates a strongly electron-withdrawing pyrazinium segment. Formation of pyrazinium ion will trigger a facile intramolecular charge transfer between the

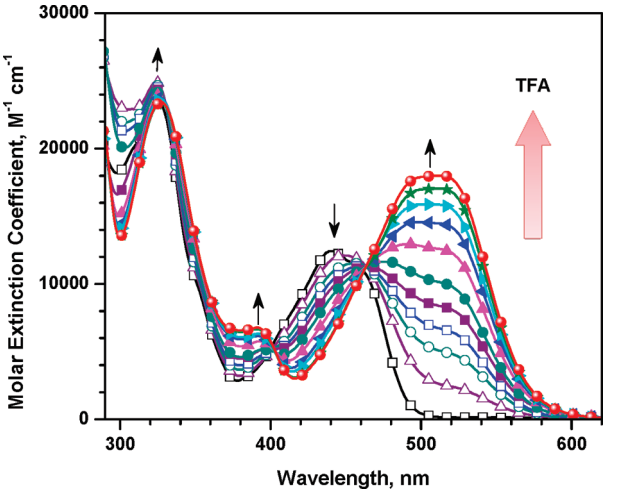

Figure 4. Absorption spectra of **3a** measured for dichloromethane solutions with different amounts of TFA.

Scheme 2. Protonation-Deprotonation Equilibria of the Dyes in the Presence of TFA

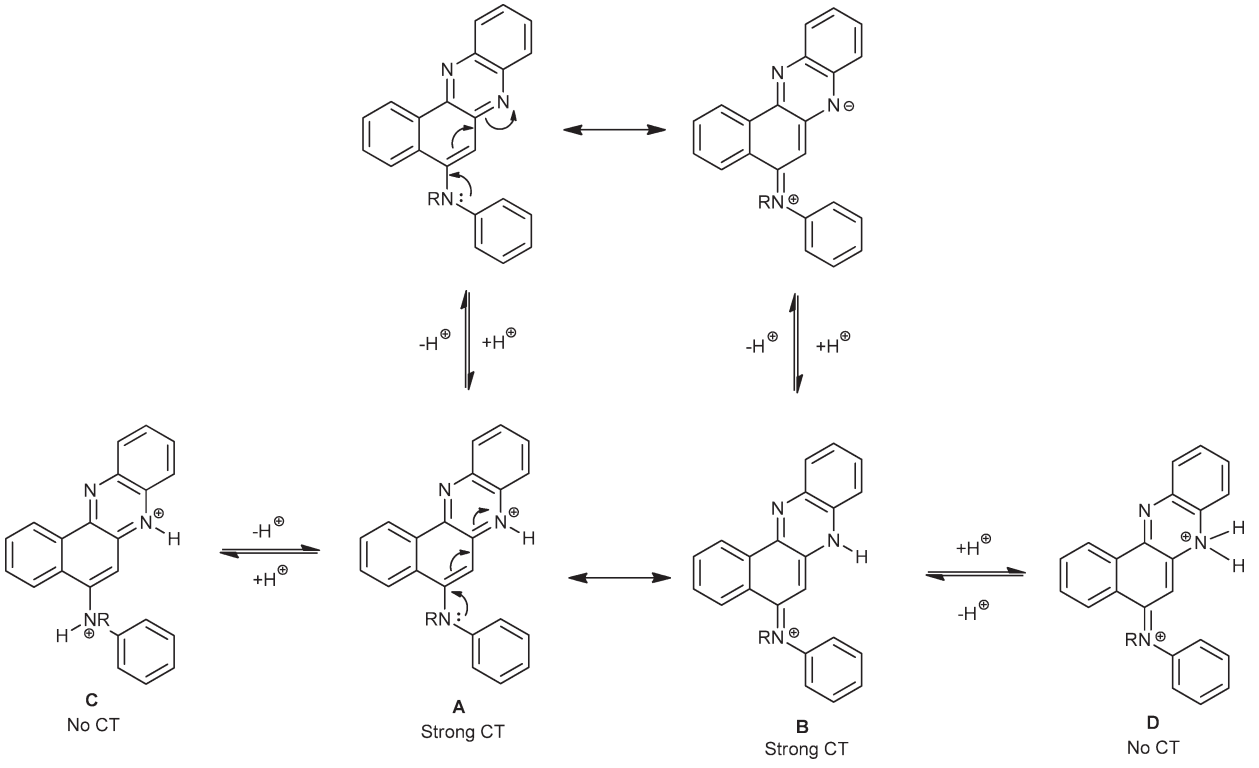

dx.doi.org/10.1021/jo200857p |*J. Org. Chem.* 2011, 76, 6134–6145

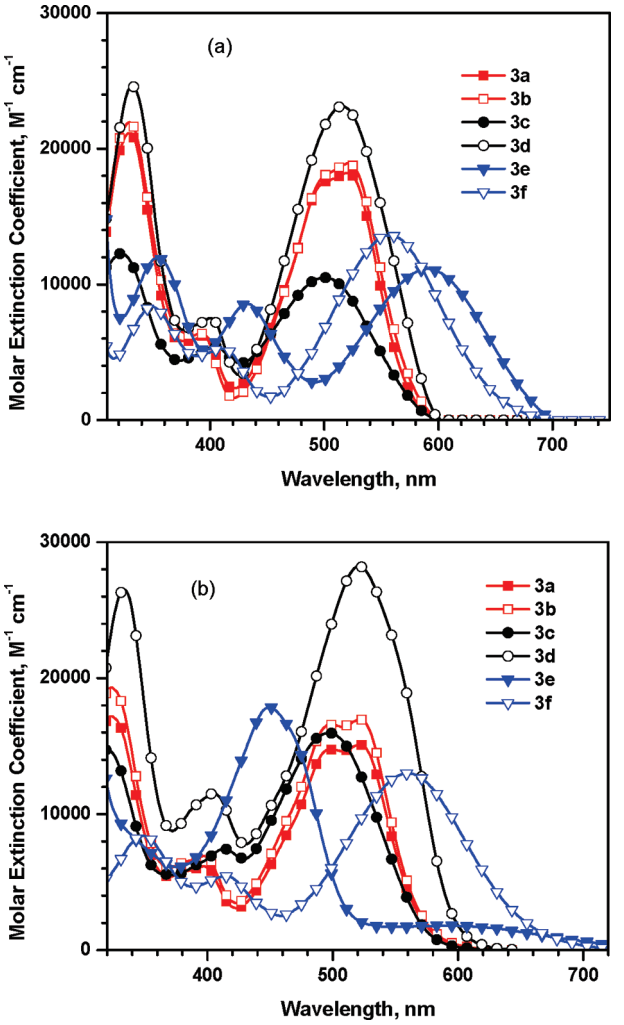

Figure 5. Absorption spectra of dyes **3a**−**f** measured in toluene solutions in the presence of (a) 10 and (b) 1000 equiv of TFA.

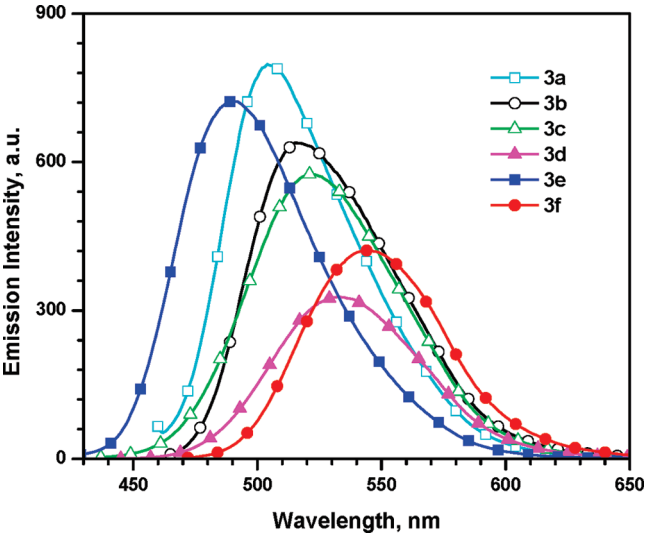

Figure 6. Fluorescence spectra of the dyes (**3a**−**f**) recorded in toluene.

amine donor and the pyrazinium acceptor segment (SCHEME 2). Protonation of nitrogen based heterocyclic components such as pyridine attached to amine donors *via* an aromatic conjugation, have been demonstrated to stabilize the LUMO and cause a dramatic red-shift in absorption.[31]

The protonation was completed on the addition of 10 equiv of TFA (Figure 5a). In DCM solutions, the compounds **3a**, **3b**, **3c**, and **3d** displayed a color change from yellow to pink-orange while for **3e** and **3f** it was from yellow to purple. The original color was regained by the addition of triethylamine which neutralized the effect arising due to the addition of TFA. The observation of one or two isosbestic points suggests the presence of the neutral and protonated forms in equilibrium and the later being predominant at higher concentrations of TFA. On the basis of the above observations, it is believed that the dyes exhibit acid−base equilibria as illustrated in SCHEME 2.

Addition of an excess of TFA (1000 equiv) led to the bleaching of the color for **3e** (Figure 5b). The absorption pattern of **3e** in the presence of excess TFA is significantly different from that observed for **3e** in the absence of TFA. The appearance of weaker charge transfer transition at the very high wavelength and broadening of signals in the proton NMR spectrum of **3e** in the presence of excess TFA are suggestive of diprotonation leading to the formation of dication "**D**". Formation of "**D**" should completely remove the donor−acceptor interactions in the molecule and the extinction of charge transfer transition. Second protonation leading to the species "**C**" or "**D**" for the dyes **3a**−**d** and **3f** is unlikely as the remaining nitrogen's will become less basic after the monoprotonation due to the severe push−pull interaction. However, due to weaker donor−acceptor interaction in **3e** between the carbazole and quinoxaline segment further protonation may be possible and would generate the species "C" which will lack ICT (see below for theoretical results).[32]

All of the dyes displayed moderately intense emission spectra for toluene solutions (Figure 6) when excited at their absorption maximum. The emission color ranged from cyan to yellowish-green depending on the nature of the amine segment (Table 2). The most blue-shifted emission profile was observed for carbazole derivative (**3e**) while the diphenylamine derivative (**3f**) displayed the longer wavelength emission in toluene solution. Among the dyes, **3c** and **3d** exhibited comparatively larger Stokes shifts in toluene indicative of the presence of more pronounced nonradiative relaxation pathways such as vibrational relaxation in these dyes originating from the flexible morpholine and piperidine units. All of the dyes were characterized by moderate fluorescence quantum yield in nonpolar solvents such as cyclohexane and toluene. A sharp decrease in the emission intensity was noticed on the addition of TFA to DCM/toluene solutions of the dyes. It appears that the protonated species, due to the presence of strong donor−acceptor interactions experiences a more pronounced dipolar relaxation from the excited state.[33]

Fluorescence spectra of the compounds were also examined in a series of solvents with varying polarity index ($E_T(30)$)[34] to identify the impact of the polarity of the solvent on the excited state of the dyes and to identify the nature of the molecules in the excited state. Representative illustrations showing the influence of the solvent polarity on the emission profile are displayed in Figure 7 for the dyes **3a**, **3c**, and **3f**. The emission profile of the dyes exhibited a positive solvatochromism with the bathochromically shifted emission maxima in the polar solvents such as dimethylformamide and acetonitrile (Table 2) which led to a gradual increase in the Stokes shift

dx.doi.org/10.1021/jo200857p |*J. Org. Chem.* 2011, 76, 6134–6145

Table 2. Emission Spectral Data for the Dyes in Different Solvents

dye	λ_{em}, nm (Φ_F, %)							Stokes shift, cm^{-1}						
	CH	CCl_4	Tol	DCM	$CHCl_3$	DMF	ACN	CH	CCl_4	Tol	DCM	$CHCl_3$	DMF	ACN
3a	474 (10)	489 (10)	504 (18)	534 (12)	524 (22)	556 (1)	557 (1)	1998	2381	2834	3695	3337	3706	4318
3b	481 (13)	498 (19)	515 (16)	554 (12)	544 (27)	485 (1)	487 (4)	2145	2544	3054	4073	3839	887	1590
3c	487 (19)	501 (10)	521 (26)	542 (11)	417 (23)	420 (6)	416 (6)	3621	4078	4787	5531	5254	6142	6308
3d	497 (13)	513 (15)	533 (25)	556 (18)	550 (27)	570 (7)	570 (7)	3803	4260	4712	5544	5292	5986	6153
3e	449 (33)	467 (18)	492 (22)	549 (17)	549 (32)	582 (2)	564 (6)	1258	2172	4489	6599	5991	7632	7084
3f	496 (20)	518 (30)	543 (27)	575 (21)	573 (34)	582 (1)	594 (9)	2210	2770	3708	4635	4382	4942	5587

on increasing the polarity. Further, the dyes exhibited linear relationship between the Stokes shift and the $E_T(30)$ parameter as illustrated in Figure 8 for the dyes **3a**, **3d**, and **3e**. The Lippert−Mataga plots[35] displayed in Figure 9 for the dyes **3d** and **3e** illustrate the typical behavior of the dyes in the excited states with the variation of orientation polarizability of the solvent. Obviously, the dyes showed different types of interactions with the nonpolar and polar solvents leading to two unique straight line correlations. This suggests that in the solvents of low polarity, a general solvation effect is present while for the polar solvents additional specific interactions such as dipole−dipole relaxation play additional role. Such dual behavior of the donor−acceptor compounds containing polyaromatic moieties in polar and nonpolar solvents has been well documented in the literature.[36]

The dyes, in general, showed moderate quantum efficiencies in nonpolar solvents such as cyclohexane and toluene; however on increasing the solvent polarity (dimethylformamide and acetonitrile), the photoluminescence yield decreased which may be ascribed to the dipole−dipole interaction of the dyes with the solvent molecules.[33]

Electrochemical Properties. The oxidation and reduction propensities of the dyes **3a**−**3f** were scrutinized by cyclic and differential pulse voltammetric methods. The redox potentials of the dyes are collected in Table 3. All of the dyes, with the exception of **3f**, showed an irreversible oxidation wave corresponding to the removal of an electron from the amine segment. The compound **3f** exhibited a quasi-reversible redox process originating from the oxidation of diphenylamine unit. It is apparent that the nature of the electronic interaction between the amine (donor) and quinoxaline (acceptor) moieties affects the oxidation potentials. As the spacer length is fixed in all the dyes, the alterations in the oxidation potentials of the dyes can be considered as the manifestations of the donor strength of the amine segment. Strong donors are expected to interact effectively with the acceptor moiety and lead to a reduction in the electrochemical bandgap. Thus lower oxidation potentials are expected for the strong donor containing derivatives **3d** and **3c** while a larger oxidation potential for the carbazole derivative **3e**. In agreement with these generalizations, the oxidation potentials of the dyes assumed the order: **3d** < **3c** < **3f** < **3a** < **3b** < **3e**. In addition, when scanning toward the negative potentials, the dyes displayed a quasi-reversible reduction process attributable to the reduction of the quinoxaline segment which follows the trend, **3d** < **3c** < **3a** ∼ **3b** < **3f** < **3e**. The easy reduction observed for the carbazole derivative (**3e**) and the difficulty of the reduction processes in **3d** and **3c** are in line with their trend in oxidation potentials. These points a weaker donor−acceptor interaction in **3e** and stronger electronic communication in the derivatives **3c** and **3d** congruent with the peak positions of the charge transitions observed for these dyes.

Thermal Properties. The thermal stability and the decomposition temperatures (T_d) of the dyes **3a**−**f** were determined by the thermal gravimetric analysis (TGA) under a nitrogen atmosphere, with a heating rate of 10 °C/min. All of the compounds exhibited a moderate T_d higher than 299 °C (Table 3). The highest thermal stability is observed for the tolylamine derivative **3b**, while the carbazole derivative **3e** displayed the lowest in the series. Generally, the carbazole based amines featuring polyaromatic hydrocarbons have been demonstrated to display high thermal robustness.[37] It is interesting to note that in violation to the belief, the carbazole derivative, **3e**, underwent a facile decomposition at a relatively low temperature probably in an attempt to relieve the steric hindrance between the benzophenazine and carbazole moieties. While such a steric crowding playing a major role in the thermal stability of the present compounds, higher decomposition temperatures observed for **3b** and **3f** are quite interesting.

Theoretical Calculations. To unravel the structure-electronic property relationship in the present compounds, we have performed DFT[38] calculations as implemented in Gaussian 09 program package.[39] We optimized the molecular structure of the dyes in the gas phase as well as in toluene using B3LYP[38] and CAM-B3LYP[40] models and 6-31G(d,p) basis set without any symmetry constraints. The optimized geometry was used for the electronic simulations where at least 10 electronic excitations were computed for each compound. The lowest energy transitions derived from the theoretical analysis along with their oscillator strengths and the compositions in terms of molecular orbital contributions are listed in Table 4. The electronic distributions in the HOMO and LUMO for the selected dyes (**3b**, **3d**, and **3f**) are shown in the Figure 10. The HOMO of these compounds is delocalized over the amine moiety, with maximum components arising from the nitrogen lone pair and/or from the π framework of the phenyl groups and is extended along the bridge to the central region of the molecule. In the LUMO-orbital, which also has π-character, there is no significant contribution from the amine segment and the electron density has shifted toward the quinoxaline moiety. From the optimized geometries, it is understandable that the slight twisting of the donor moiety from the benzophenazine plane hinders the electronic interaction between the donor and acceptor fragments. It is interesting to compare the calculated electronic structures with the electro-optical data of the dyes. First, we notice that the distribution of HOMO and LUMO are not well separated within the molecule and a significant overlap is present. This indicates that the HUMO-LUMO transitions cannot be considered as a pure charge transfer transition and is may be

dx.doi.org/10.1021/jo200857p |J. Org. Chem. 2011, 76, 6134–6145

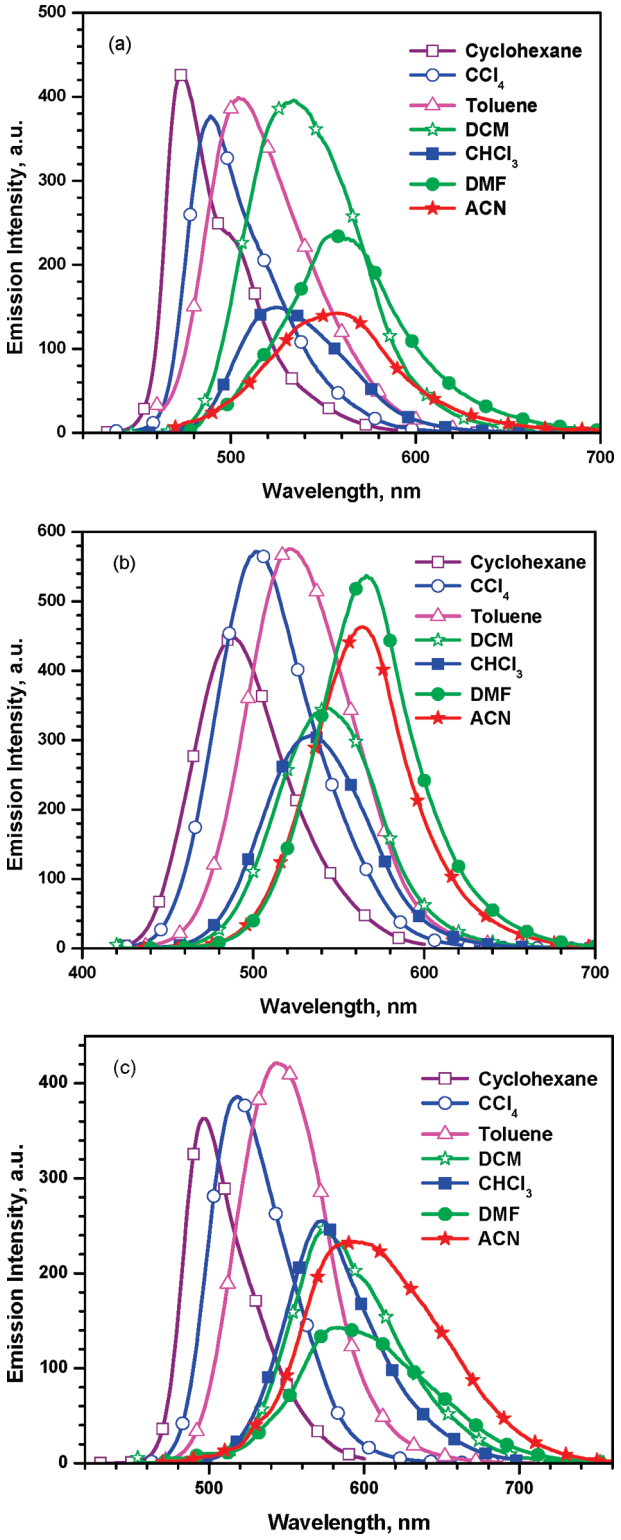

Figure 7. Emission spectra of (a) **3a**, (b) **3c**, and (c) **3f** recorded in different solvents.

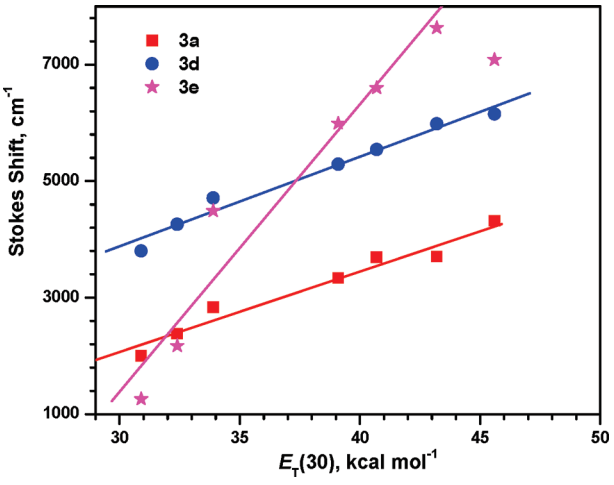

Figure 8. Variation of Stokes shift with the solvent polarity parameter ($E_T(30)$) for the dyes **3a**, **3d**, and **3e**.

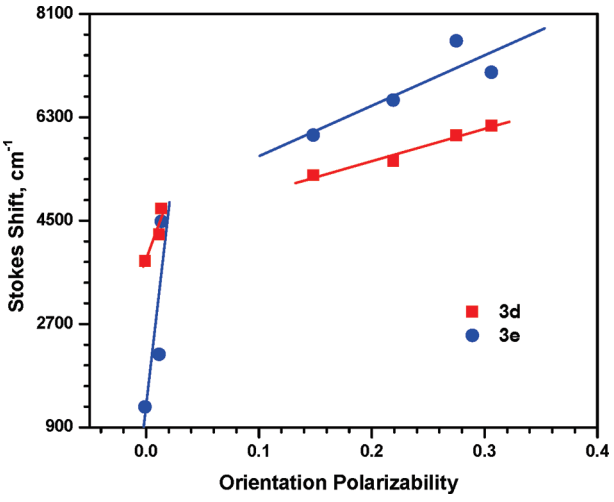

Figure 9. Lippart–Mataga plots observed for the dyes (a) **3d** and (b) **3e**.

treated as $\pi-\pi^*$ transitions with prominent charge transfer contribution.[41] The calculated transitions for the HOMO–LUMO in gas phase at the B3LYP level are closely matching to the experimentally observed optical data for the dyes in toluene with the exception of **3e**. A slight red-shifted profile predicted for **3f** may be attributed to the stronger donor strength of diphenylamine unit which may lead to an extended charge transfer interaction that cannot be precisely modeled in the DFT computations. However, the trend observed for the absorption maxima of the dyes in toluene is well supported by the theoretical computations.

In order to identify the effect of protonation on the optical properties, we have optimized the geometry of the protonated forms of the dyes also. Except for slight structural variations no significant alternations in the geometry were observed due to protonation. The HOMO of the dyes **3a**, **3b**, **3c**, and **3d** on protonation has shown a change in the electron distribution away from the quinoxaline segment, while in the HOMO of **3f** the movement of electron density toward the quinoxaline segment is noticed. However, no noteworthy changes in the electron distribution are observed for the LUMO of the dyes due to protonation. All of these observations suggest that protonation on the quinoxaline segment enhances the electron-accepting ability and drifts the electron-density toward it and the effect is highly dependent on the donor strength of the amine. Stronger donor such as diphenylamine pushes more electron density in

dx.doi.org/10.1021/jo200857p |J. Org. Chem. 2011, 76, 6134–6145

Table 3. Electrochemical and Thermal Data of the Dyes

dye	E_{ox} (ΔE_p), mV[d]	E_{red} (ΔE_p), mV [d]	optical edge, nm	HOMO, eV	LUMO, eV	E_{0-0}, eV	T_{onset}, °C	T_d, °C
3a	873	−1837	500	5.673	2.963	2.479	282	339
3b	903	−1840	520	5.703	2.959	2.384	351	421
3c	696	−1892 (128)	482	5.481	2.908	2.573	294	362
3d	592	−1908 (111)	500	5.372	2.892	2.480	275	350
3e	1084	−1745 (131)	474	5.739	3.061	2.678	244	299
3f	705 (101)	−1823 (136)	534	5.396	2.974	2.422	318	389

Table 4. Computed Vertical Transitions and Their Oscillator Strengths (f) for the Dyes and Their Protonated Forms

	λ_{max} (calc.) nm, (f)					
	B3LYP		CAM B3LYP			
			neutral		protonated	
dye	neutral (gas)	protonated (gas)	gas	tol	gas	tol
3a	448.1 (0.1668)	471.9 (0.3511)	365.8 (0.2870)	377.3 (0.4245)	564.6 (0.1220)	546.3 (0.1996)
3b	455.5 (0.1685)	842.3 (0.0783)	368.8 (0.2884)	380.0 (0.4209)	575.0 (0.1201)	553.6 (0.1957)
3c	408.5 (0.1519)	684.3 (0.0705)	342.9 (0.2504)	352.0 (0.4028)	503.8 (0.1264)	487.2 (0.2061)
3d	414.0 (0.1569)	686.7 (0.0806)	346.1 (0.2644)	356.2 (0.4072)	517.2 (0.1305)	501.2 (0.2090)
3e	497.2 (0.0460)	740.4 (0.2506)[a]	351.4 (0.1559)	352.0 (0.2627)	687.8 (0.07160)	572.3 (0.0879)
3f	492.1 (0.1618)	547.3 (0.4208)	373.2 (0.3003)	382.4 (0.4230)	620.1 (0.1433)	578.5 (0.2145)

[a] for the diprotonated species: 467.6 (0.2169).

view of the stronger demand from the pyrazinium fragment. Higher wavelength vertical transitions were predicted for the protonated dyes, which is in agreement with the observed values. For the diprotonated species of **3e** no ICT at higher wavelength was observed which supports the color bleaching occurred at higher concentrations of TFA. Calculated dipole moments of protonated species are higher than the neutral dyes which corroborates the nonemissive nature of the dyes in solution due to the more effective solvent induced dipolar relaxation mechanisms.

CONCLUSIONS

In summary we have developed a synthetic strategy for the hitherto unknown amine-substituted benzo[a]phenazines starting from 1,2-naphthoquinones by employing simple addition and condensation reactions with the suitable amines. The amine-substituted benzo[*a*]phenazines displayed rich optical properties in the ground and excited states. Although the absorption spectra of the dyes were not influenced by the nature of the solvents, addition of TFA led to the preferential protonation of at the quinoxaline segment. This has resulted in an interesting acidochromism. In view of the importance of the acidochromic samples in the sensor industry we have studied the electronic structure of the dyes by DFT computations. From that the red-shifted absorption peak observed for the dyes were identified to be originating from a $\pi-\pi^*$ transition with minor contribution from the charge transfer between the donor and acceptor fragments. The qualitative trends observed in the optical properties were supported by the theoretical computations and pointing that the electronic structure in small molecules with weak donor−acceptor interactions can be modeled with accuracy using DFT theory.

The emission spectra of the dyes showed positive solvatochromism suggestive of a more polarized excited state stabilized by polar solvents. The dyes were also characterized by their efficient redox properties and moderate thermal stability. All of the compounds displayed a quasi-reversible reduction couple which is tunable by the nature of the amine segment. The potential electro-optical properties realized for this new class of dipolar compounds makes them attractive functional materials.

EXPERIMENTAL SECTION

General. ^{1}H and ^{13}C spectra were recorded on a 500 MHz spectrometer. Mass spectra were collected on an ESI TOF high-resolution mass spectrometer. Electronic absorption spectra were measured on a spectrometer using the dichloromethane or toluene solutions. Emission spectra were recorded using a spectrofluorimeter operating at the room temperature (~32 °C). Emission quantum yields were obtained by using coumarin-6 (Φ_F = 0.78 in ethanol) as reference. Cyclic voltammetry experiments were performed using an electrochemical analyzer with a conventional three-electrode configuration consisting of a glassy carbon working electrode, platinum auxiliary electrode, and a nonaqueous $Ag/AgNO_3$ reference electrode. The $E_{1/2}$ values were determined as $1/2(E^p_a + E^p_c)$, where E^p_a and E^p_c are the anodic and cathodic peak potentials, respectively. All potentials reported are not corrected for the junction potential. The solvent in all experiments was CH_2Cl_2, and the supporting electrolyte was 0.1 M tetrabutylammonium perchlorate. DSC measurements were carried out on a differential scanning calorimeter at a heating rate of 10 °C/min and a cooling rate of 30 °C/min under nitrogen atmosphere. TGA measurements were performed on a thermogravimetric analyzer at a heating rate of 10 °C/min under a flow of nitrogen.

Synthesis of Naphthoquinone Derivatives (2a−f). A mixture of naphthoquinone (12.0 mmol) and corresponding amine

dx.doi.org/10.1021/jo200857p |*J. Org. Chem.* 2011, 76, 6134–6145

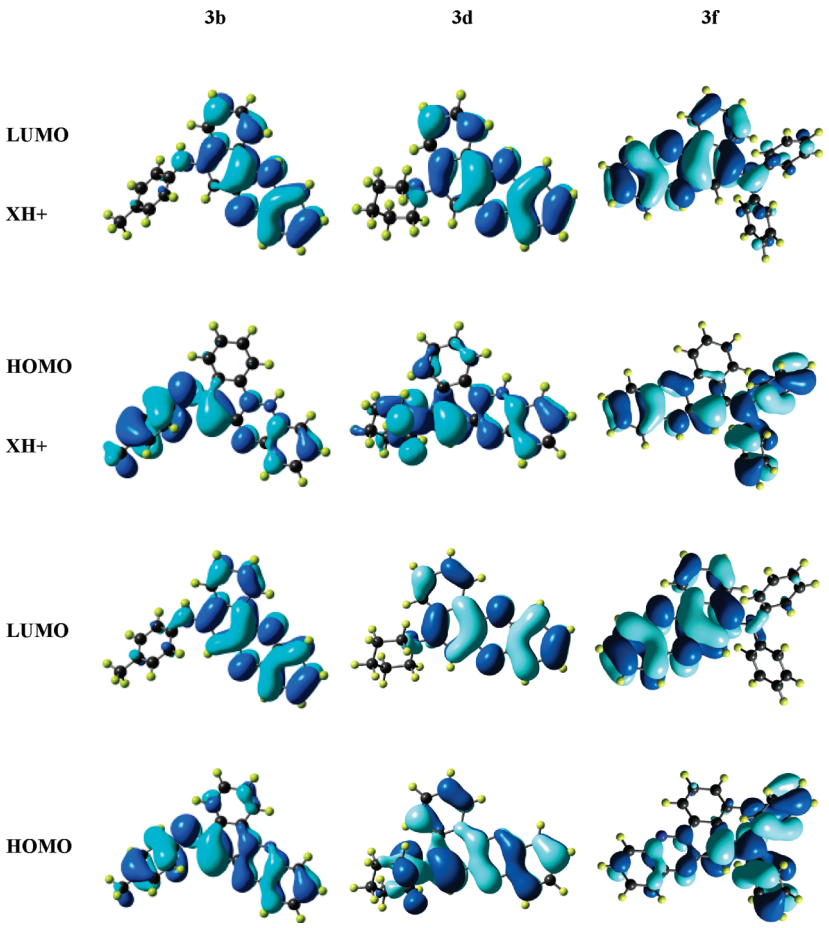

Figure 10. Electronic distributions observed for the frontier molecular orbitals of the dyes **3b**, **3d**, and **3f**.

(12.0 mmol) was heated in chloroform (20 mL) at 60 °C with stirring for 30 min. After cooling to room temperature, it was poured to beaker containing hexane (100 mL) and agitated for 10 min. The precipitate formed was filtered and washed thoroughly with hexane. Further purification was effected by chromatography on silica gel using hexane/dichloromethane mixture (1:1) as eluant.

4-(Phenylamino)naphthalene-1,2-dione ***(2a)***. **2a** was synthesized from naphthoquinone and aniline by following the general procedure described above. Blackish red solid. Yield: 60%. mp 240−242 °C; IR (KBr, cm^{-1}): 3317 (ν_{N-H}), 1695 ($\nu_{C=O}$). ^1H NMR ($CDCl_3$, 500.13 MHz): δ 6.68 (s, 1 H), 6.91−6.93 (m, 1 H), 7.02−7.05 (m, 1 H), 7.07−7.08 (m, 1 H), 7.10−7.13 (m, 1 H), 7.35−7.39 (m, 2 H), 7.63−7.66 (m, 1 H), 7.75 (dt, J = 7.5 Hz, 1.5 Hz, 1 H), 8.22−8.24 (m, 1 H), 8.55 (d, J = 7.5 Hz, 1 H). ^{13}C NMR (DMSO- d_6, 125.770 MHz): δ 186.3, 159.8, 159.5, 144.7, 139.5, 137.0, 136.7, 134.6, 134.2, 133.3, 131.2, 131.0, 130.4, 129.3, 128.7, 125.5, 105.7. Anal. Calcd for $C_{16}H_{11}NO_2$: C, 77.10; H, 4.45; N, 5.62. Found: C, 76.82; H, 4.34; N, 5.45.

4-(p-Toluidino)naphthalene-1,2-dione ***(2b)***. **2b** was synthesized from naphthoquinone and *p*-toluidine by following the general procedure described above. Reddish brown solid. Yield: 45%. mp 242−244 °C; IR (KBr, cm^{-1}): 3301 (ν_{N-H}), 1699 ($\nu_{C=O}$). ^1H NMR ($CDCl_3$, 500.13 MHz): δ 2.39 (d, J = 6.0 Hz, 3 H), 6.66 (s, 1 H), 6.81 (dd, J = 6.5 Hz, 2.0 Hz, 1 H), 7.06 (s, 1 H), 7.17−7.22 (m, 2 H), 7.65−7.68 (m, 2 H), 7.75−7.77 (m, 1 H), 8.20 (dd, J = 7.5 Hz, 1.5 Hz, 1 H), 8.55 (dd, J = 8.0 Hz, 1.0 Hz, 1 H). ^{13}C NMR (DMSO- d_6, 125.770 MHz): δ 181.7, 176.2, 155.1, 136.8, 135.6, 134.8, 133.8, 132.0, 131.3, 130.4, 128.6, 126.4, 124.3, 120.7, 104.4, 100.7, 21.1. Anal. Calcd for $C_{17}H_{13}NO_2$: C, 77.55; H, 4.98; N, 5.32. Found: C, 77.31; H, 4.84; N, 5.19.

4-Morpholinonaphthalene-1,2-dione ***(2c)***. **2c** was synthesized from naphthoquinone and morpholine by following the general procedure described above. Brown solid. Yield: 51%. mp 145−146 °C; IR (KBr, cm^{-1}): 1687 ($\nu_{C=O}$). ^1H NMR ($CDCl_3$, 500.13 MHz): δ 3.36 (t, J = 5.0 Hz, 4 H), 3.93(t, J = 5.0 Hz, 4 H), 6.00 (s, 1 H), 7.53−7.57 (m, 2 H), 7.63−7.67 (m, 1 H), 8.13 (dd, J = 7.5 Hz, 1.0 Hz, 1 H). ^{13}C NMR ($CDCl_3$, 100.62 MHz): δ 180.3, 178.7, 163.3, 134.1, 132.0, 130.9, 129.7, 126.6, 109.8, 66.1, 51.6. Anal. Calcd for $C_{14}H_{13}NO_3$: C, 69.12; H, 5.39; N, 5.76. Found: C, 68.90; H, 5.24; N, 5.63.

4-(9H-Carbazol-9-yl)naphthalene-1,2-dione ***(2e)***. **2e** was synthesized from naphthoquinone and carbazole by following the general procedure described above. Dark red solid. Yield: 55%. mp 218−220 °C; IR (KBr, cm^{-1}): 1695 ($\nu_{C=O}$). ^1H NMR ($CDCl_3$, 500.13 MHz): δ 7.68 (dd, J = 8.0 Hz, 0.5 Hz, 1 H), 7.82−7.89 (m, 5 H), 7.93−7.96 (m, 2 H), 8.00−8.03 (m, 1 H), 8.11−8.14 (m, 1 H), 8.66 (d, J = 7.5 Hz, 2 H), 8.79−8.81 (m, 1 H). ^{13}C NMR ($CDCl_3$, 125.770 MHz): δ 180.5, 178.7, 151.6, 140.2, 135.3, 132.1, 131.9, 131.5, 130.6, 127.9, 126.7, 126.0, 124.7, 121.6, 120.7, 111.5. Anal. Calcd for $C_{22}H_{13}NO_2$: C, 81.72; H, 4.05; N, 4.33. Found: C, 81.54; H, 3.91; N, 4.14.

4-Diphenylamino-[1,2]naphthoquinone ***(2f)***. **2f** was synthesized from naphthoquinone and diphenylamine by following the general procedure described above. Dark red solid. Yield: 75%. mp 216−218 °C; IR (KBr, cm^{-1}): 1635 ($\nu_{C=O}$). ^1H NMR ($CDCl_3$, 500.13 MHz): δ 6.01 (s, 1 H), 6.44 (s, 1 H), 7.04−7.08 (m, 1 H), 7.12−7.15 (m, 2 H), 7.19−7.21 (m, 2 H), 7.33−7.38 (m, 4 H), 7.48−7.50 (m, 1 H), 7.53 (dt, J = 7.5 Hz, 1.5 Hz, 1 H), 7.60 (dt, J = 7.5 Hz, 1.5 Hz, 1 H), 8.20 (dd, J = 7.5 Hz, 1.5 Hz, 1 H). ^{13}C NMR ($CDCl_3$, 100.624 MHz): δ 180.5, 180.0, 156.9, 145.7, 141.3, 135.3,

dx.doi.org/10.1021/jo200857p |*J. Org. Chem.* 2011, 76, 6134–6145

134.9, 131.9, 130.6, 130.5, 129.9, 129.64, 129.56, 127.8, 126.6, 126.3, 122.8, 119.9, 115.9. Anal. Calcd for $C_{22}H_{15}NO_2$: C, 81.21; H, 4.65; N, 4.30. Found: C, 81.05; H, 4.49; N, 4.17.

N-Phenylbenzo[a]phenazin-5-amine ***(3a)***. A mixture of 4-(phenylamino)naphthalene-1,2-dione (**2a**, 2 g, 8.0 mmol), *o*-phenylenediamine (0.86 g, 8.0 mmol) in chloroform (20 mL) was heated to reflux in presence of *p*-toluene sulfonic acid (10 mg) with efficient stirring for 5 h. On removal of the volatiles, a dark brown solid was obtained. This was purified by chromatography on silica gel using hexane/chloroform mixture (3:2) as eluant. Yellow solid. Yield: 88%. mp 218−220 °C; IR (KBr, cm^{-1}): 3419 (ν_{N-H}). ^1H NMR ($CDCl_3$, 500.13 MHz): δ 6.49 (s, 1 H), 7.17−7.20 (m, 1 H), 7.38−7.45 (m, 4 H), 7.53 (s, 1 H), 7.72−7.79 (m, 2 H), 7.86−7.89 (m, 2 H), 8.10−8.12 (m, 2 H), 8.27−8.29 (m, 1 H), 9.51−9.53 (m, 1 H). ^1H NMR ($CDCl_3$ + TFA, 500 MHz): δ 6.92 (s, 1 H), 7.43−7.40 (m, 1 H), 7.55−7.53 (m, 2 H), 7.63−7.59 (m, 2 H), 7.84−7.81 (m, 1 H), 7.97−7.90 (m, 2 H), 8.08−8.02 (m, 2 H), 8.31−8.28 (m, 1 H), 8.70−8.67 (m, 1 H), 9.24−9.19 (m, 1 H), 10.25 (s, 1 H). ^{13}C NMR ($CDCl_3$, 125.77 MHz): δ 145.4, 143.8, 143.3, 140.8, 140.6, 140.5, 131.9, 129.9, 129.8, 129.7, 128.42, 128.38, 128.3, 128.0, 126.4, 124.1, 122.6, 120.5, 104.6. HRMS calcd. for $C_{22}H_{16}N_3$ [M + H] *m/z* 322.1344, Found: 322.1346. Anal. Calcd for $C_{22}H_{15}N_3$: C, 82.22; H, 4.70; N, 13.08. Found: C, 82.03; H, 4.56; N, 12.89.

5-p-Tolylbenzo[a]phenazine ***(3b)***. It was prepared in 86% yield from **2b** as described above for **3a**. Brown solid. mp 220−222 °C;IR (KBr, cm^{-1}): 3387 (ν_{N-H}). ^1H NMR ($CDCl_3$, 500.13 MHz): δ 2.39 (s, 3H), 6.48 (s, 1 H), 7.22−7.24 (m, 2 H), 7.27−7.28 (m, 2 H), 7.39 (s, 1 H), 7.69−7.72 (m, 1 H), 7.74−7.77 (m, 1 H), 7.83−7.87 (m, 2 H), 8.07−8.09 (m, 2 H), 8.25−8.27 (m, 1 H), 9.49−9.51 (m, 1 H). ^1H NMR ($CDCl_3$ + TFA, 500.13 MHz): δ 2.44 (s, 3 H), 6.79 (s, 1 H), 7.43 (s, 4 H), 7.83−7.80 (m, 1 H), 7.87 (d, *J* = 8.5 Hz, 1 H), 7.94 (t, *J* = 7.5 Hz, 1 H), 8.05−8.00 (m, 2 H), 8.27−8.25 (m, 1 H), 8.68−8.66 (m, 1 H), 9.17−9.15 (m, 1 H), 10.35 (s, 1 H). ^{13}C NMR ($CDCl_3$, 125.75 MHz): δ 145.5, 144.5, 140.5, 137.8, 134.2, 131.8, 130.3, 129.8, 129.6, 128.3, 128.2, 127.8, 126.3, 123.4, 120.3, 103.5, 21.0. HRMS calcd. for $C_{23}H_{18}N_3$ [M + H] *m/z* 336.1501, Found: 336.1505. Anal. Calcd for $C_{23}H_{17}N_3$: C, 82.36; H, 5.11; N, 12.53, Found: C, 82.12; H, 4.97; N, 12.35.

5-Morpholinobenzo[a]phenazine ***(3c)***. **3c** was obtained as yellow solid (55%) from **2c** by following the procedure described above for **3a**. mp 160−162 °C; IR (KBr, cm^{-1}): 1624 ($\nu_{C=N}$). ^1H NMR ($CDCl_3$, 500.13 MHz): δ 3.31 (s, 4 H), 4.05 (t, *J* = 4.5 Hz, 4 H), 7.44 (s, 1 H), 7.79−7.85 (m, 4 H), 8.19−8.23 (m, 2 H), 8.32−8.41 (m, 1 H), 9.44−9.46 (m, 1 H). ^1H NMR ($CDCl_3$ + TFA, 500.13 MHz): δ 3.75 (t, *J* = 4.5 Hz, 4 H), 4.19 (m, 4 H), 7.36 (s, 1 H), 8.03−7.95 (m, 3 H), 8.14−8.08 (m, 2 H), 8.18 (d, *J* = 8.0 Hz, 2 H), 8.50 (dd, *J* = 7.5, 1.0 Hz, 1 H), 9.41 (dd, *J* = 8.0, 1.5 Hz, 1 H). ^{13}C NMR ($CDCl_3$, 100.62 MHz): δ 153.2, 144.6, 143.0, 141.3, 141.2, 132.2, 130.4, 129.9, 129.6, 129.5, 128.8, 128.6, 128.0, 126.0, 124.2, 112.8, 67.1, 53.0. HRMS calcd. for $C_{20}H_{18}N_3O$ [M + H] *m/z* 316.1450, Found 316.1449. Anal. Calcd for $C_{20}H_{17}N_3O$: C, 76.17; H, 5.43; N, 13.32. Found: C, 75.95; H, 5.28; N, 13.15.

5-(Piperidin-1-yl)benzo[a]phenazine ***(3d)***. A mixture of 1,2-naphthoquinone (1.58 g, 10 mmol) and piperidine (0.87 g, 10 mmol) in chloroform was stirred at 60 °C for 45 min. After cooling, *o*-phenylene diamine (1.08 g, 10 mmol) and *p*-toluene sulfonic acid (10 mg) were added and refluxed for 6 h. After the completion of the reaction, the solvent was removed by rotary evaporation to obtain a brown solid. It was subjected to column chromatography on silica gel using hexane/dichloromethane mixture (3:2) as eluant. Yellow solid. Yield: 80%. mp 157−160 °C; IR (KBr, cm^{-1}): 1620 ($\nu_{C=N}$). ^1H NMR ($CDCl_3$, 500.13 MHz): δ 1.74 (s, 2 H), 1.89−1.93 (m, 4 H), 3.25 (s, 4 H), 7.40 (s, 1 H), 7.76−7.83 (m, 4 H), 8.17−8.21 (m, 2 H), 8.30−8.32 (m, 1 H), 9.41−9.44 (m, 1 H). ^1H NMR ($CDCl_3$ + TFA, 500.13 MHz): δ 1.92 (s, 2 H), 2.07 (s, 4 H), 3.87 (s, 4 H), 7.56−7.55 (m, 1 H), 8.06−8.02 (m, 3 H), 78.12 (s, 2 H), 8.22−8.21 (m,1 H), 8.53−8.52 (m, 1 H), 9.43 (d, *J* = 8.0 Hz, 1 H). ^{13}C NMR ($CDCl_3$, 125.75 MHz): δ 154.8, 145.0, 143.0, 141.4, 141.0, 132.0, 131.1, 129.8, 129.4, 128.5, 127.8, 125.9, 124.6, 112.2, 54.9, 29.7, 26.3, 24.5. HRMS calcd. for $C_{21}H_{20}N_3$ [M + H] *m/z* 314.1657, Found: 314.1663. Anal. Calcd for $C_{21}H_{19}N_3$: C, 80.48; H, 6.11; N, 13.41. Found: C, 80.33; H, 5.97; N, 13.15.

5-(9H-Carbazol-9-yl)benzo[a]phenazine ***(3e)***. **3e** was synthesized from **2e** by following a procedure similar to that described above for **3a**. Yellow solid. Yield: 45%. mp 224−225 °C; IR (KBr, cm^{-1}): 1622 ($\nu_{C=N}$). ^1H NMR ($CDCl_3$, 500.13 MHz): δ 7.19−7.21 (m, 2 H), 7.33−7.40 (m, 5 H), 7.58−7.61 (m, 1 H), 7.85−7.88 (m, 1 H), 7.92−7.95 (m, 2 H), 8.23−8.25 (m, 3 H), 8.30−8.32 (m, 1 H), 8.45−8.47 (m, 1 H) 9.60−9.62 (m, 1 H). ^1H NMR ($CDCl_3$ + TFA, 500.13 MHz): δ 7.24−7.22 (m, 2 H), 7.43−7.40 (m, 4 H), 7.89−7.87 (m, 2 H), 8.14−8.10 (m, 1 H), 8.28−8.21 (m, 4 H), 8.39 (s, 1 H), 8.50−8.49 (m, 1 H), 8.73−8.71 (m, 1 H), 9.66−9.65 (m, 1 H). ^{13}C NMR ($CDCl_3$, 125.75 MHz): δ 143.4, 143.3, 142.5, 142.4, 141.7, 138.9, 132.4, 130.9, 130.5, 130.5, 130.1, 129.9, 129.4, 128.8, 127.8, 126.2, 126.0, 124.7, 123.6, 120.5, 120.4. 110.5. HRMS calcd. for $C_{28}H_{18}N_3$ [M + H] *m/z* 396.1501, Found: 396.1514. Anal. Calcd for $C_{28}H_{17}N_3$: C, 85.04; H, 4.33; N, 10.63. Found: C, 84.79; H, 4.17; N, 10.51.

N,N-Diphenylbenzo[a]phenazin-5-amine ***(3f)***. **3f** was synthesized from **2f** by following a procedure similar to that described above for **3a**. Yellow solid. Yield: 70%. mp 200−202 °C; IR (KBr, cm^{-1}): 1623 ($\nu_{C=N}$). ^1H NMR ($CDCl_3$, 500.13 MHz): δ 5.93 (s, 1 H), 7.00−7.03(m, 1 H), 7.21−7.25 (m, 4 H), 7.33−7.36 (m, 2 H), 7.53−7.55 (m, 2 H), 7.73−7.77 (m, 1 H), 7.81−7.85 (m, 1 H), 7.85−7.89 (m, 2 H), 7.94 (s, 1 H), 8.07 (d, *J* = 8.0 Hz, 1 H), 8.26−8.29 (m, 1 H), 8.37−8.40 (m, 1 H), 9.55 (dd, *J* = 8.0 Hz, 1.0 Hz, 1 H).^{1H} NMR ($CDCl_3$ + TFA, 500.13 MHz): δ 7.04−7.03 (m, 4 H), 7.19−7.15 (m, 2 H), 7.28 (t, *J* = 7.5 Hz, 3 H), 7.52−7.49 (m, 1 H), 7.83−7.73 (m, 3 H), 7.90−7.87 (m, 1 H), 8.16−8.13 (m, 1 H), 8.32 (d, *J* = 8.0 Hz, 1 H), 9.29−9.27 (d, *J* = 8.0 Hz, 1 H). ^{13}C NMR ($CDCl_3$, 125.77 MHz): δ 149.1, 148.3, 144.3, 143.0, 141.6, 130.1, 130.0, 129.8, 129.7, 129.6, 129.5, 129.4, 129.3, 128.8, 128.0, 125.8, 125.72, 125.67, 124.7, 123.7, 123.3, 121.2, 118.3, 114.0. HRMS calcd. for $C_{28}H_{20}N_3$ [M + H] *m/z* 398.1657, Found: 398.1658. Anal. Calcd for $C_{28}H_{19}N_3$: C, 84.61; H, 4.82; N, 10.57. Found: C, 84.46; H, 4.70; N, 10.34.

Computational Methods. The ground state geometry of the compounds at the gas phase were optimized using the density functional theory method with the B3LYP functional[38] in conjugation with the basis set 6-31G(d, p) as implemented in the Gaussian 09 package.[39] The default options for the self-consistent field (SCF) convergence and threshold limits in the optimization were used. The electronic transitions were calculated using the time-dependent DFT (B3LYP) theory and the 6-31G (d, p) basis set. Even though the time-dependent DFT method less accurately describes the states with charge-transfer nature, the qualitative trends in the TDDFT results can still offer correct physical insights. At least 10 excited states were calculated for each molecule.

Crystallographic Measurements. Red crystals of **6** were grown from CH_2Cl_2/*n*-hexane at room temperature. Data collection was carried out on a single crystal X-ray diffractometer at room temperature. MoK_α radiation (λ = 0.71073 Å) was used. The unit-cell parameters were obtained by least-squares fit to the automatically centered settings for reflections. Data were collected in $\omega/2\theta$ scan mode. Corrections were made for Lorentz and polarization effects. All calculations were performed using the WINGX software package.[42] Structure solution was done by direct method and refined by a full-matrix least-squares method on F^2 (*F*: structure factor). The monoclinic space group $P12_1/n1$ was determined from the systematic absence of specific reflections; successful refinement of the structure confirmed the space group assignment. The dichloromethane solvent present in the crystal and the butyl fragment were found to be disordered and this explains the observed high *R* values.

dx.doi.org/10.1021/jo200857p |*J. Org. Chem.* 2011, 76, 6134–6145

■ ASSOCIATED CONTENT

Supporting Information. ^{1}H and ^{13}C NMR and optical spectra of the newly synthesized compounds, crystallographic data for the compound **2e**, Cartesian coordinates of the optimized structures. This material is available free of charge via the Internet at http://pubs.acs.org.

■ AUTHOR INFORMATION

Corresponding Author

*Tel: +91-1332-285376; Fax: +91-1332-286202; E-mail: krjt8fcy@iitr.ernet.in.

■ ACKNOWLEDGMENT

We thank the Department of Science and Technology (DST), New Delhi, India for financial support (Grant No. SR/S1/OC-11/2007). Single crystal X-ray facility at the Sophisticated Analytical Instrumentation Facility of the Indian Institute of Technology Madras is also acknowledged for X-ray diffraction data collection. Prof. R. Barthwal of the Department of Biotechnology is thanked for allowing us to use the NMR facility in the Institute Instrumentation Centre.

■ REFERENCES

(1) (a) Leung, M. K.; Chang, C.-C.; Wu, M.-H.; Chuang, K.-H.; Lee, J.-H.; Shieh, S.-J.; Lin, S.-C.; Chiu, C.-F. *Org. Lett.* **2006**, *8*, 2623. (b) Chen, C. T. *Chem. Mater.* **2004**, *16*, 4389.

(2) (a) Yan, Q.; Zhou, Y.; Ni, B. B.; Ma, Y. G.; Wang, J.; Pei, J.; Cao, Y. *J. Org. Chem.* **2008**, *73*, 5328. (b) Murphy, A. R.; Frèchet, J. M. J. *Chem. Rev.* **2007**, *107*, 1066.

(3) (a) Hochbaum, A. I.; Yang, P. *Chem. Rev.* **2010**, *110*, 527. (b) Gregg, B. A. *J. Phys. Chem. B* **2003**, *107*, 4688.

(4) (a) Thomas, S.W., III; Joly, G. D.; Swager, T. M. *Chem. Rev.* **2007**, *107*, 1339.

(5) (a) Baheti, A.; Singh, P.; Thomas, K. R. J.; Hsu, Y. -C.; Ho, K. -C.; Lin, J. T. *Dyes Pigm.* **2011**, *91*, 33. (b) Hauck, M.; Turdean, R.; Memminger, K.; Schonhaber, J.; Rominger, F.; Muller, T. J. J. *J. Org. Chem.* **2010**, *75*, 8591. (c) Baheti, A.; Tyagi, P.; Thomas, K. R. J.; Hsu, Y. C.; Lin, J. T. *J. Phys. Chem. C* **2009**, *113*, 8541. (d) Kivala, M.; Diederich, F. *Acc. Chem. Res.* **2009**, *42*, 235. (e) Oliva, M. M.; Casado, J.; Raposo, M. M. M.; Fonseca, A. M. C.; Hartmann, H.; Hernandez, V.; Navarrete, J. T. L. *J. Org. Chem.* **2006**, *71*, 759. (f) Lambert, C.; Schelter, J.; Fiebig, T.; Mank, D.; Trifonov, A. *J. Am. Chem. Soc.* **2005**, *127*, 10600. (g) Velusamy, M.; Thomas, K. R. J.; Lin, J. T.; Hsu, Y.-C.; Ho, K.-C. *Org. Lett.* **2005**, *7*, 1899. (h) Thomas, K. R. J.; Lin, J. T.; Velusamy, M.; Tao, Y.-T.; Chuen, C.-H. *Adv. Funct. Mater.* **2004**, *14*, 83. (i) Seo, J.; Kim, S.; Park, S. Y. *J. Am. Chem. Soc.* **2004**, *126*, 11154. (j) Raimundo, J. M.; Blanchard, P.; Gallego-Planas, N.; Mercier, N.; Ledoux-Rak, I.; Hierle, R.; Roncali, J. *J. Org. Chem.* **2002**, *67*, 205. (k) Breitung, E. M.; Shu, C. F.; McMahon, R. J. *J. Am. Chem. Soc.* **2000**, *122*, 1154.

(6) (a) Hagfeldt, A.; Boschloo, G.; Sun, L.; Kloo, L.; Pettersson, H. *Chem. Rev.* **2010**, *110*, 6595. (b) Ning, Z.; Tian, H. *Chem. Commun* **2009**, 5483. (c) Yoshida, J. I.; Kataoka, K.; Horcajada, R.; Nagaki, A. *Chem. Rev.* **2008**, *108*, 2265. (d) Thomas, K. R. J.; Lin, J. T.; Tao, Y.-T.; Ko, C.-W. *Chem. Mater.* **2002**, *14*, 1354.

(7) (a) Mohamad, D. K.; Fischereder, A.; Yi, H. N.; Cadby, A. J.; Lidzey, D. G.; Iraqi, A. *J. Mater. Chem.* **2011**, *21*, 851. (b) Koumura, N.; Wang, Z.-S.; Mori, S.; Miyashita, M.; Suzuki, E.; Hara, K. *J. Am. Chem. Soc.* **2008**, *130*, 4202. (c) Thomas, K. R. J.; Lin, J. T.; Tao, Y.-T.; Ko, C.-W. *J. Am. Chem. Soc.* **2001**, *123*, 3852.

(8) (a) Cao, D.; Peng, J.; Hong, Y.; Fang, X.; Wang, L.; Meier, H. *Org. Lett.* **2011**, *13*, 1610. (b) Park, P.; Kim, B.; Lee, C.; Hyun, A.; Jang, S.; Lee, J.-H.; Gal, Y.-S.; Kim, T. H.; Kim, K.-S.; Park, J. *J. Phys. Chem. C* **2011**, *115*, 4843. (c) Li, D. M.; Lv, L. F.; Sun, P. P.; Zhou, W.; Wang, P.; Wu, J.; Kan, Y.; Zhou, H.; Tian, Y. *Dyes Pigm.* **2009**, *83*, 180.

(9) (a) Zhang, J.; Deng, D.; He, C.; He, Y.; Zhang, M.; Zhang, Z.-G.; Zhang, Z.; Li, Y. *Chem. Mater.* **2011**, *23*, 817. (b) Baheti, A.; Singh, P.; Thomas, K. R. J. *Dyes Pigm.* **2011**, *88*, 195. (c) Bader, M. M.; Pham, P. T. T.; Elandaloussi, E. *Cryst. Growth Des.* **2010**, *10*, 5027. (d) Tang, X.; Liu, W.; Wu, J.; Lee, C.-S.; You, J.; Wang, P. *J. Org. Chem.* **2010**, *75*, 7273. (e) Du, C.; Chen, J.; Guo, Y.; Lu, K.; Ye, S.; Zheng, J.; Liu, Y.; Shuai, Z.; Yu, G. *J. Org. Chem.* **2009**, *74*, 7322. (f) Raposo, M. M. M.; Sousa, A. M. R. C.; Kirsch, G.; Cardoso, P.; Belsley, M.; Gomes, E. D. M.; Fonseca, A. M. C. *Org. Lett.* **2006**, *8*, 3681. (g) Roquet, S.; Cravino, A.; Leriche, P.; Alévêque, O.; Frère, P.; Roncali, J. *J. Am. Chem. Soc.* **2006**, *128*, 3459.

(10) (a) Chen, B. S.; Chen, D. Y.; Chen, C. L.; Hsu, C.-W.; Hsu, H.-C.; Wu, K.-L.; Liu, S.-H.; Chou, P.-T.; Chi, Y. *J. Mater. Chem.* **2011**, *21*, 1937. (b) Ning, Z.; Fu, F.; Tian, H. *Energy Environ. Sci.* **2010**, *3*, 1170. (c) Marinado, T.; Nonomura, K.; Nissfolk, J.; Karlsson, M. K.; Hagberg, D. P.; Sun, L.; Mori, S.; Hagfeldt, A. *Langmuir* **2010**, *26*, 2592. (d) Ooyama, Y.; Harima, Y. *Eur. J. Org. Chem.* **2009**, 2903.

(11) (a) Zhao, Z.-H.; Jin, H.; Zhang, Y.-X.; Shen, Z.; Zou, D.-C.; Fan, X.-H. *Macromolecules* **2011**, *44*, 1405. (b) Miguel, M. D.; Álvaro, M.; Ding, J.; Garc$_1$a, H. *J. Phys. Chem. C* **2010**, *114*, 14255. (c) Kamtekar, K. T.; Wang, C. S.; Bettington, S.; Batsanov, A. S.; Perepichka, I. F.; Bryce, M. R.; Ahn, J. H.; Rabinal, M.; Petty, M. C. *J. Mater. Chem.* **2006**, *16*, 3823. (d) Thomas, K. R. J.; Lin, J. T.; Tao, Y.-T.; Chuen, C.-H. *Chem. Mater.* **2004**, *16*, 5437. (e) Mochizuki, H.; Hasui, T.; Kawamoto, M.; Shiono, T.; Ikeda, T.; Adachi, C.; Taniguchi, Y.; Shirota, Y. *Chem. Commun.* **2000**, 1923. (f) Tamoto, N.; Adachi, C.; Nagai, K. *Chem. Mater.* **1997**, *9*, 1077.

(12) (a) Beaujuge, P. M.; Subbiah, J.; Choudhury, K. R.; Ellinger, S.; McCarley, T. D.; So, F.; Reynolds, J. R. *Chem. Mater.* **2010**, *22*, 2093. (b) Wang, J.-L.; Xiao, Q.; Pei, J. *Org. Lett.* **2010**, *12*, 4164. (c) Wang, J.-L.; Tang, Z.-M.; Xiao, Q.; Ma, Y.; Pei, J. *Org. Lett.* **2009**, *11*, 863. (d) Sonar, P.; Singh, S. P.; Leclere, P.; Surin, M.; Lazzaroni, R.; Lin, T. T.; Dodabalapur, A.; Sellinger, A. *J. Mater. Chem.* **2009**, *20*, 3228.

(13) (a) Huang, T.-H.; Whang, W.-T.; Shen, J. Y.; Wen, Y.-S.; Lin, J. T.; Ke, T.-H.; Chen, L.-Y.; Wu, C.-C. *Adv. Funct. Mater.* **2006**, *16*, 1449. (b) Hancock, J. M.; Gifford, A. P.; Zhu, Y.; Lou, Y.; Jenekhe, S. A. *Chem. Mater.* **2006**, *18*, 4924. (c) Huang, T.-H.; Lin, J.-T. *Chem. Mater.* **2004**, *16*, 5387.

(14) (a) Son, H.-J.; Han, W.-S.; You, D.-H.; Min, K.-T.; Kwon, S.-N.; Ko, J.; Kang, S. O. *J. Org. Chem.* **2009**, *74*, 3175. (b) Son, H.-J.; Han, W.-S.; Wee, K.-R.; Yoo, D.-H.; Lee, J.-H.; Kwon, S.-N.; Ko, J.; Kang, S. O. *Org. Lett.* **2008**, *10*, 5401.

(15) (a) Xu, X.; Yu, G.; Chen, S.; Di, C.; Liu, Y. *J. Mater. Chem.* **2008**, *18*, 299. (b) Kulkarni, A. P.; Zhu, Y.; Babel, A.; Wu, P.-T.; Jenekhe, S. A. *Chem. Mater.* **2008**, *20*, 4212. (c) Chen, S.; Xu, X.; Liu, Y.; Qiu, W.; Yu, G.; Wang, H.; Zhu, D. *J. Phys. Chem. C* **2007**, *111*, 1029. (d) Kulkarni, A. P.; Tonzola, C. J.; Babel, A.; Jenekhe, S. A. *Chem. Mater.* **2004**, *16*, 4556. (e) Schmitz, C.; Pösch, P.; Thelakkat, M.; Schmidt, H.-W.; Montali, A.; Feldman, K.; Smith, P.; Weder, C. *Adv. Funct. Mater.* **2001**, *11*, 41.

(16) (a) Thomas, K. R. J.; Lin, J. T.; Tao, Y. T.; Chuen, C. H. *Chem. Mater.* **2002**, *14*, 2796. (b) Thomas, K. R. J.; Lin, J. T.; Tao, Y. T.; Chuen, C. H. *J. Mater. Chem.* **2002**, *12*, 3516.

(17) (a) Cornil, J.; Beljonne, D.; Parente, V.; Lazzaroni, R.; Brédas, J. L. In *Handbook of Oligo- and Polythiophenes*; Fichou, D., Ed.; Wiley-VCH: Weinheim, Germany, 1999. (b) Cornil, J.; Beljonne, D.; Brédas, J. L. In *Electronic Materials: The Oligomer Approach*; Müllen, K., Wegner, G., Eds.; Wiley-VCH: Weinheim, Germany, 1998. (c) Mishra, A.; Ma, C. Q.; Bauerle, P. *Chem. Rev.* **2009**, *109*, 1141. (d) Robertson, N.; McGowan, C. A. *Chem. Soc. Rev.* **2003**, *32*, 96. (e) Otsubo, T.; Aso, Y.; Takimiya, K. *J. Mater. Chem.* **2002**, *12*, 2565. (f) Otsubo, T.; Aso, Y.; Takimiya, K. *Bull. Chem. Soc. Jpn.* **2001**, *74*, 1789.

(18) (a) Mikroyannidis, J. A.; Tsagkournos, D. V.; Sharma, S. S.; Vijay, Y. K.; Sharma, G. D. *J. Mater. Chem.* **2011**, *21*, 4679. (b) Sonar, P.; Singh, S. P.; Li, Y.; Soh, M. S.; Dodabalapur, A. *Adv. Mater.* **2010**, *22*, 5409.

(19) (a) Lin, T.-C.; Huang, Y.-J.; Chen, Y.-F.; Hu, C.-L. *Tetrahedron* **2010**, *66*, 1375. (b) Wei, Y.; Samori, S.; Tojo, S.; Fujitsuka, M.; Lin, J.-S.;

Chen, C.-T.; Majima, T. *J. Am. Chem. Soc.* **2009**, *131*, 6698. (c) Izadyar, A.; Omer, K. M.; Liu, Y.; Chen, S.; Xu, X.; Bard, A. J. *J. Phys. Chem. C* **2008**, *112*, 20027. (d) Zhan, X.; Liu, Y.; Wu, X.; Wang, S.; Zhu, D. *Macromolecules* **2002**, *35*, 2529. (e) Thomas, K. R. J.; Velusamy, M.; Lin, J. T.; Chuen, C. H.; Tao, Y. T. *Chem. Mater.* **2005**, *17*, 1860.

(20) (a) Matsidik, R.; Mamtimin, X.; Mi, H. Y.; Nurulla, I. *J. Appl. Poly. Sci.* **2010**, *118*, 74. (b) Mikroyannidis, J. A.; Kabanakis, A. N.; Kumar, A.; Sharma, S. S.; Vijay, Y. K.; Sharma, G. D. *Langmuir* **2010**, *26*, 12909. (c) Udum, Y. A.; Durmus, A.; Gunbas, Gorkem, E.; Toppare, L. *Org. Electron.* **2008**, *9*, 501.

(21) (a) Li, H.; Tam, T. L.; Lam, Y. M.; Mhaisalkar, S. G.; Grimsdale, A. C. *Org. Lett.* **2011**, *13*, 46. (b) Lee, Y.; Russell, T. P.; Jo, W. H. *Org. Electron.* **2010**, *11*, 846.

(22) (a) Mondal, R.; Kob, S.; Bao, Z. *J. Mater. Chem.* **2010**, *20*, 10568. (b) Mondal, R.; Miyaki, N.; Becerril, H. A.; Norton, J. E.; Parmer, J.; Mayer, A. C.; Tang, M. L.; Bredas, J. L.; McGehee, M. D.; Bao, Z. A. *Chem. Mater.* **2009**, *21*, 3618. (c) Wen, L.; Nietfeld, J. P.; Amb, C. M.; Rasmussen, S. C. *J. Org. Chem.* **2008**, *73*, 8529. (d) Özen, A. S.; Atilgan, C.; Sonmez, G. *J. Phys. Chem. C* **2007**, *111*, 16362. (e) Thomas, K. R. J.; Lin, J. T.; Tao, Y. T.; Chuen, C. H. *Adv. Mater.* **2002**, *14*, 822.

(23) (a) Robins, K. A.; Jang, K.; Cao, B.; Lee, D.-C. *Phys. Chem. Chem. Phys.* **2010**, *12*, 12727. (b) Leng, S.; Chan, L. H.; Jing, J.; Hu, J.; Moustafa, R. M.; Horn, R. M. V.; Graham, M. J.; Sun, B.; Zhu, M.; Jeong, K. U.; Kaafarani, B. R.; Zhang, W.; Harris, F. W.; Cheng, S. Z. D. *Soft Matter* **2010**, *6*, 100. (c) Aldakov, D.; Palacios, M. A.; Anzenbacher, P., Jr. *Chem. Mater.* **2005**, *17*, 5238.

(24) Thomas, K. R. J.; Tyagi, P. *J. Org. Chem.* **2010**, *75*, 8100.

(25) (a) Lavaggi, M. L.; Cabrera, M.; Aravena, M. A.; Olea-Azar, C.; de Ceráin, A. L.; Monge, A.; Pachón, G.; Cascante, M.; Bruno, A. M.; Pietrasanta, L. I.; González, M.; Cerecetto, H. *Bioorg. Med. Chem.* **2010**, *18*, 4433. (b) Velusamy, M.; Shen, J.-Yi; Lin, J. T.; Lin, Y.-C.; Hsieh, C.-C.; Lai, C.-H.; Lai, C.-W.; Ho, M.-L.; Chen, Y.-C.; Chou, P.-T.; Hsiao, J.-K. *Adv. Funct. Mater.* **2009**, *19*, 2388.

(26) (a) Dou, C.; Han, L.; Zhao, S.; Zhang, H.; Wang, Y. *J. Phys. Chem. Lett.* **2011**, *2*, 666. (b) Zucchero, A. J.; Tolosa, J.; Tolbert, L. M.; Bunz, U. H. F. *Chem. Eur. J. -A* **2009**, *15*, 13075.

(27) Singh, M. W.; Karmakar, A.; Barooah, N.; Baruah, J. B. *Beilstein J. Org. Chem.* **2007**, *3*, 10.

(28) (a) Eicher, T.; Haupmann, S. *The Chemistry of Heterocycles*, Second ed.; Wiley-VCH Verlag GmbH & Co. KGaA: New York, 2003. (b) Smith, M. B.; March, J. *Advanced Organic Chemistry: Reactions, Mechanisms, and Structure*, 6th ed.; Wiley-Interscience: New York, 2007.

(29) (a) Wang, T. T.; Chung, S. M.; Wu, F. I.; Shu, C. F.; Diau, E. W. G. *J. Phys. Chem. B* **2005**, *109*, 23827. (b) Grabowski, Z. R.; Rotkiewicz, K. *Chem. Rev.* **2003**, *103*, 3899. (c) Gulbinas, V.; Markovitsi, D.; Gustavsson, T.; Karpicz, R.; Veber, M. *J. Phys. Chem. A* **2000**, *104*, 5181.

(30) (a) Murugan, N. A. *J. Phys. Chem. B* **2011**, *115*, 1056. (b) Ikeda, S.; Toganoh, M.; Easwaramoorthi, S.; Lim, J. M.; Kim, D.; Wang, H. F. *J. Org. Chem.* **2010**, *75*, 8637. (c) Z., S.; Li, F.-Y.; Huang, C.-H. *J. Phys. Chem. B* **2001**, *105*, 9210.

(31) (a) Tolosa, J.; Solntsev, K. M.; Tolbert, L. M.; Bunz, U. H. F. *J. Org. Chem.* **2010**, *75*, 523. (b) Grabiec, E.; Kurcok, M.; Schab-Balcerzak, E. *J. Phys. Chem. A* **2009**, *113*, 1481. (c) Spitler, E. L.; Shirtcliff, L. D.; Haley, M. M. *J. Org. Chem.* **2007**, *72*, 86. (d) Spitler, E. L.; McClintock, S. P.; Haley, M. M. *J. Org. Chem.* **2007**, *72*, 6692.

(32) (a) Yang, C. H.; Liao, S.-H.; Sun, Y.-K.; Chuang, Y.-Y.; Wang, T.-L.; Shieh, Y.-T.; Lin, W.-C. *J. Phys. Chem. C* **2010**, *114*, 21786. (b) Holzapfel, M.; Lambert, C. *J. Phys. Chem. C* **2008**, *112*, 1227. (c) Huang, S.-T.; Hsu, Y.-C.; Yen, Y.-S.; Chou, H. H.; Lin, J. T.; Chang, C.-W.; Hsu, C.-P.; Tsai, C.; Yin, D.-J. *J. Phys. Chem. C* **2008**, *112*, 19739.

(33) (a) Kokado, K.; Chujo, Y. *J. Org. Chem.* **2011**, *76*, 316. (b) Moyano, F.; Quintana, S. S.; Falcone, R. D.; Silber, J. J.; Correa, N. M. *J. Phys. Chem. B* **2009**, *113*, 4284. (c) Haldar, S.; Chattopadhyay, A. *J. Phys. Chem. B* **2007**, *111*, 14436. (d) Wong, K.-T.; Fang, F.-C.; Cheng, Y.-M.; Chou, P.-T.; Lee, G.-H.; Wang, Y. *J. Org. Chem.* **2004**, *69*, 8038.

(34) Reichardt, C. *Chem. Rev.* **1994**, *94*, 2319.

(35) (a) Dias, F. B.; Pollock, S.; Hedley, G.; Palsson, L.-O.; Monkman, A.; Perepichka, I. I.; Perepichka, I. F.; Tavasli, M.; Bryce, M. R. *J. Phys. Chem. B* **2006**, *110*, 19329. (b) Krishnamoorthy, G.; Dogra, S. K. *J. Org. Chem.* **1999**, *64*, 6566. (c) Mataga, N.; Chosrowjan, H.; Taniguchi, S. *J. Photochem. Photobiol. C: Photochem. Rev.* **2005**, *6*, 37. (d) Von Lippert, E. Z. *Naturforsch A: Phys. Sci.* **1955**, *10*, 541. (e) Mataga, N.; Kaifu, Y.; Koizumi, M. *Bull. Chem. Soc. Jpn.* **1955**, *28*, 690. (f) Von Lippert, E. Z. *Electrochem.* **1957**, *61*, 962.

(36) (a) Moss, K. C.; Bourdakos, K. N.; Bhalla, V.; Kamtekar, K. T.; Bryce, M. R.; Fox, M. A.; Vaughan, H. L.; Dias, F. B.; Monkman, A. P. *J. Org. Chem.* **2010**, *75*, 6771. (b) Brombosz, S. M.; Zucchero, A. J.; McGrier, P. L.; Bunz, U. H. F. *J. Org. Chem.* **2009**, *74*, 8909. (c) Bortolus, P.; Galiazzo, G.; Gennari, G.; Monti, S. *Photochem. Photobiol. Sci.* **2002**, *1*, 412.

(37) (a) Sasabe, H.; Kido, J.; He, J. *Chem. Mater.* **2011**, *23*, 621. (b) Liu, H.; Dai, Y.; Ou, X.; Wang, J.; Tao, S.; Zhang, X.; Wang, P.; Ma, D. *J. Phys. Chem. C* **2009**, *113*, 6761. (c) Iraqi, A.; Wataru, I. *Chem. Mater.* **2004**, *16*, 442.

(38) Lee, C.; Yang, W.; Parr, R. G. *Phys. Rev. B* **1988**, *37*, 785.

(39) Frisch, M. J.; Trucks, G. W.; Schlegel, H. B.; Scuseria, G. E.; Robb, M. A.; Cheeseman, J. R.; Scalmani, G.; Barone, V.; Mennucci, B.; Petersson, G. A.; Nakatsuji, H.; Caricato, M.; Li, X.; Hratchian, H. P.; Izmaylov, A. F.; Bloino, J.; Zheng, G.; Sonnenberg, J. L.; Hada, M.; Ehara, M.; Toyota, K.; Fukuda, R.; Hasegawa, J.; Ishida, M.; Nakajima, T.; Honda, Y.; Kitao, O.; Nakai, H.; Vreven, T.; Montgomery, J. A., Jr.; Peralta, J. E.; Ogliaro, F.; Bearpark, M.; Heyd, J. J.; Brothers, E.; Kudin, K. N.; Staroverov, V. N.; Kobayashi, R.; Normand, J.; Raghavachari, K.; Rendell, A.; Burant, J. C.; Iyengar, S. S.; Tomasi, J.; Cossi, M.; Rega, N.; Millam, N. J.; Klene, M.; Knox, J. E.; Cross, J. B.; Bakken, V.; Adamo, C.; Jaramillo, J.; Gomperts, R.; Stratmann, R. E.; Yazyev, O.; Austin, A. J.; Cammi, R.; Pomelli, C.; Ochterski, J. W.; Martin, R. L.; Morokuma, K.; Zakrzewski, V. G.; Voth, G. A.; Salvador, P.; Dannenberg, J. J.; Dapprich, S.; Daniels, A. D.; Farkas, Ö .; Foresman, J. B.; Ortiz, J. V.; Cioslowski, J.; Fox, D. J. *Gaussian 09, revision A.02*; Gaussian, Inc.: Wallingford, CT, 2009.

(40) Yanai, T.; Tew, D. P.; Handy, N. C. *Chem. Phys. Lett.* **2004**, *393*, 51.

(41) (a) Lu, M.; Liang, M.; Han, H.-Y.; Sun, Z.; Xue, S. *J. Phys. Chem. C* **2011**, *115*, 274. (b) Xu, W.; Peng, B.; Chen, J.; Liang, M.; Cai, F. *J. Phys. Chem. C* **2008**, *112*, 874. (c) Hagberg, D. P.; Marinado, T.; Karlsson, K. M.; Nonomura, K.; Qin, P.; Boschloo, G.; Brinck, T.; Hagfeldt, A.; Sun, L. *J. Org. Chem.* **2007**, *72*, 9550.

(42) Farrugia, L. J. *J. Appl. Crystallogr.* **1999**, *32*, 837.